REVIEWS OF MODERN PHYSICS VOLUME 16, NUMBERS 3 AND 4 JULY-OCTOBER, 1944

The Absorption Laws for Gases in the Infra-Red

J. RUD NIELSEN
Department of Physics, University of Oklahoma, Norman, Oklahoma

V. THORNTON AND E. BROCK DALE
Phillips Petroleum Company, Bartlesville, Oklahoma

INTRODUCTION

WHEN a parallel beam of monochromatic radiation of intensity I_0 enters a homogeneous absorbing material, the radiation transmitted through a layer of thickness l will have the intensity

$$I=I_0e^{-kl}, \tag{1}$$

where k is a positive constant called the *absorption coefficient* of the material. This law was discovered about two hundred years ago by J. H. Lambert.[1] A century later A. v. Beer[2] found that in many cases the absorption coefficient is proportional to the concentration of the absorbing material. If the absorbing material is a mixture of two or more components, the absorption coefficient is given, according to Beer, by a linear expression

$$k=c_1\epsilon_1+c_2\epsilon_2+c_3\epsilon_3+\cdots, \tag{2}$$

where $c_1, c_2, c_3\cdots$ are the concentrations of the various components, and $\epsilon_1, \epsilon_2, \epsilon_3\cdots$ are characteristic constants, the so-called *extinction coefficients*, for these components.

Lambert's law is readily derived on the assumption that each infinitesimally thin layer of the absorbing material absorbs an amount of radiation which is proportional to the thickness of the layer and to the intensity of the monochromatic radiation reaching it. Beer's law follows from the assumption that each molecule of the absorbing material absorbs the radiation independently of every other molecule. Since this assumption is not always valid, and since it is impossible to work with strictly monochromatic light, deviations from Beer's and Lambert's laws are observed in many cases.

The rapidly multiplying applications of infra-red absorption spectra to the analysis of mixtures of chemical compounds has presented an urgent need for a renewed study of the absorption laws holding for different types of infra-red absorption bands. The practical spectroscopist must know how the extinctions he measures depend upon the concentrations of the compounds which he wants to determine. He should know, also, how to choose the experimental conditions so as to obtain extinctions which are, as closely as possible, linear functions of the concentrations; for, when that is the case, i.e., when Beer's law holds, an n-component mixture can be analyzed simply by measuring the extinction at n wave-lengths and solving a set of n linear equations; whereas when appreciable deviations from Beer's law occur, more elaborate procedures must be employed.

Deviations from the simple absorption laws are observed particularly with gases and with mixtures of polar liquids. Only the case of gases will be considered here.

PREVIOUS EXPERIMENTAL WORK

Deviations from Beer's law for gases in the infra-red were first observed by K. Angström[3–7] more than 40 years ago. He used an absorption tube having two compartments of unequal length which were separated by a rocksalt plate and connected by a capillary glass tube with stopcock. After evacuation of both compartments, the shorter compartment was filled with carbon dioxide; a parallel beam of radiation was passed through the cell; and the bolometer deflection measured. The stopcock was then opened to permit the gas to expand and fill both compartments, and the deflection was measured again. Although the thickness of the absorbing gas was increased exactly in the proportion that the density was decreased, so that the absorption should remain unchanged if Beer's law held, Angström found in all cases a considerable decrease in the absorption as the pressure was decreased. When dry and carbon dioxide-free air was let into the cell until the original pressure was restored, the absorption rose to its original value. Angström surmised that the increase in absorption with increasing pressure at constant product of partial pressure and path length is caused by a broadening with pressure of individual absorption lines or bands, then unobserved.

Cl. Schaefer[8] was the first to make such measurements with more or less monochromatic radiation. He observed the absorption of carbon dioxide at 2.7 and 4.3μ and obtained results similar to those of Angström. Schaefer also found that as the thickness of the absorbing layer was increased at constant pressure of the absorbing gas the absorption would increase less than is predicted by Lambert's law and approach a maximum value of less than 100 percent. He concluded from this that the absorption bands are made up of many fine lines separated by regions in which there is no absorption.

H. Rubens and E. Ladenburg[9] found that the extinction coefficient of carbon dioxide at 14.7μ varies greatly with the total pressure. Angström's work was extended by J. Koch[10] and especially by Eva v. Bahr[11–15] who studied the principal absorption maxima of a number of different gases in the rocksalt region. Some of her results are shown in Fig. 1. The percent absorption of a constant amount of the absorbing gas mixed with different amounts of a non-absorbing gas is plotted against the total pressure. The non-absorbing gas was hydrogen in most cases, air and oxygen in others. It is seen that the absorption increases first rapidly and then slowly with increasing total pressure until a maximum is reached. For a few absorbing gases, such as the vapors of methyl alcohol, methyl, and ethyl ether, and benzene, Miss v. Bahr found no increase in the absorption with the addition of a foreign gas. She attempted to correlate the value of the total pressure at which a compound reaches its maximum absorption with the size of its molecules and found that the larger the molecules are the lower is the total pressure required to give maximum absorption. This led her to conclude that the effect is caused by molecular collisions. C. Füchtbauer[16] suggested that the pressure effect consists solely in the broadening of the individual absorption lines to be expected from Lorentz's theory of damping by molecular collisions.[17]

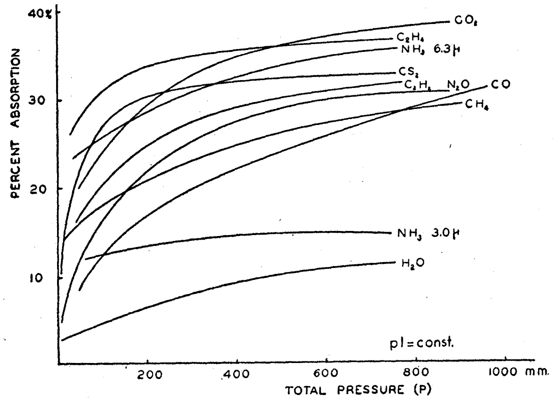

FIG. 1. Percent absorption of constant amounts of various absorbing gases plotted against the total pressure P. The total pressure was increased by adding non-absorbing gases, such as hydrogen, oxygen or air, while the product, pl, of the partial pressure of the absorbing gas and the cell length was kept constant (Eva v. Bahr).

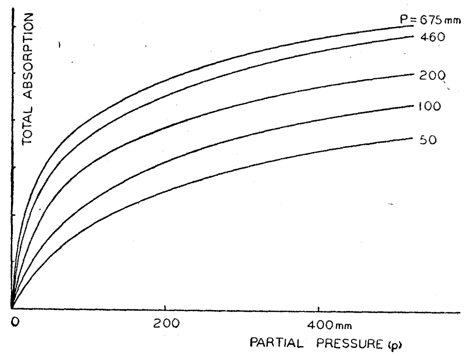

FIG. 2. Working curves for carbon dioxide in air. The total absorption, $A=\int(1-T_i)d\nu_i$, for the 4.3μ CO_2 band is plotted against the partial pressure of CO_2 for five different values of the total pressure P (M. Wimmer).

G. Hertz[18] found that the pressure effect for carbon dioxide depends somewhat upon the nature of the non-absorbing gas added to increase the total pressure. This was confirmed by M. Wimmer[19] who made a careful study of the influence of different foreign gases upon the unresolved 4.3μ band of carbon dioxide. Wimmer applied his results to the problem of determining the CO_2 content of air. Some of his working curves are shown in Fig. 2. The total absorption (see Eq. (11)), increases less than proportional to the partial pressure of the absorbing gas and depends greatly upon the total pressure.

W. Lasareff[20] investigated the influence of argon, air, hydrogen chloride, and hydrogen bromide upon the intensities of the 3.5μ band of HCl, the 3.9μ band of HBr, and the 2.7μ band of

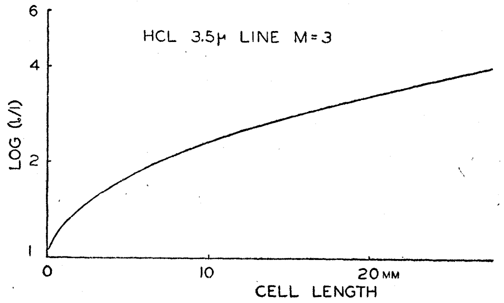

FIG. 3. Extinction, log (I_0/I), at center of line $m=3$ in the 3.5μ band of HCl is plotted against cell length at constant pressure. The line is curved rather than straight, in (apparent) violation of Lambert's law (D. G. Bourgin).

CO_2. He found that the dipole gases HCl and HBr exert about twice as great an influence upon the observed extinctions as do argon and air.

W. Grasse[21] studied the influence of several foreign gases upon the unresolved 3.5μ band of hydrogen chloride. He devised a method for estimating the broadening of the individual absorption lines from the observed increase in the absorption and calculated the distance between the centers of colliding molecules. Except for helium, these "optical diameters" are greater than those derived from the kinetic theory. Similar results were obtained by P. C. Cross and Farrington Daniels[22] who found a linear relationship between the optical and the kinetic theory diameters.

In the investigations mentioned so far, the spectral resolution was too small to resolve the rotational structure of the bands. However, in 1925 G. Becker[23] studied the effect of pressure upon the individual lines of the 3.46μ band of hydrogen chloride. The observed increase in extinction coefficient was greater when the hydrogen chloride was compressed than when air was added. Becker showed that his results could be accounted for as resulting from a broadening of the absorption lines.

Somewhat later D. G. Bourgin[24] made a careful study of the intensity distribution in the rotational lines of the 3.46μ HCl band. He measured the extinction at an individual absorption line for different thicknesses of the absorbing layer and found considerable deviation from Lambert's law. He also studied the extinction as a function of the pressure and found considerable deviation from Beer's law. Two of his curves are shown in Figs. 3 and 4. The similarity between the second of these curves and the working curves obtained by Wimmer is striking.

The intensity distribution in a line in the 1.75μ band of hydrogen chloride at pressures up to 12 atmospheres was investigated by H. Becker[25] who concluded that broadening of the lines was caused partly by Lorentz collision damping and partly by a resonance coupling.

Observations on the broadening with pressure of molecular absorption lines in the photographic infra-red have been reported by R. M. Badger and J. L. Binder,[26] G. Herzberg and J. W. T. Spinks,[27] S. D. Cornell and W. W. Watson,[28] and S. D. Cornell.[29]

Studies by H. W. Kussmann[30] of the influence of foreign gases upon the pure rotation lines of hydrogen chloride and by J. Kühne[31] of the pure rotation spectrum of water vapor in the region from 40 to 90μ gave results similar to those obtained for vibration-rotation bands.

The bearing of the failure of Beer's law upon industrial infra-red spectroscopy has recently been discussed briefly by R. R. Brattain, R. S. Rasmussen, and A. M. Cravath[32] and by R. B. Barnes, R. C. Gore, U. Liddel, and V. Z. Williams.[33, 34]

THEORETICAL

The theoretical understanding of the failure of the simple absorption laws for gases in the infra-red began with Angström's assumption that ab-

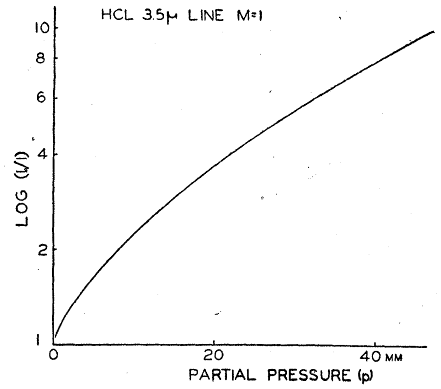

FIG. 4. Extinction, log (I_0/I), at center of line $m=1$ in the 3.5μ band of HCl plotted against pressure at constant cell length (D. G. Bourgin).

sorption bands consist of individual lines which are broadened by pressure and with Schaefer's explanation of the observed deviations from Lambert's law as caused by the limited resolution of the spectrometers used.

G. L. Gouy[35] seems to have been the first to recognize that even the sharpest spectral lines have a finite width. Lord Rayleigh[36] called attention to the Doppler effect as a cause of line broadening. M. Planck[37,38] pointed out that moving electrified particles suffer a damping caused by their own radiation field, and this effect was treated in detail by W. C. Mandersloot.[39] In 1906 H. A. Lorentz[17] showed that if the vibrations of the electrons are interrupted or suffer considerable change in phase when atoms or molecules collide, a damping and a line broadening similar to those produced by a frictional force proportional to the electronic velocity will result. J. Holtsmark[40] developed a theory for the broadening of spectral lines by intermolecular Stark effect, and Holtsmark[41] and L. Mensing[42] took the first steps toward a theoretical treatment of the broadening of spectral lines caused by resonance coupling between like atoms or molecules.

A new basis for such problems was provided by V. Weisskopf and E. Wigner[43] who applied Dirac's theory of radiation to explain the natural line width. V. Weisskopf[44] and H. Margenau and W. W. Watson[45] have given comprehensive accounts of the quantum-mechanical theories of spectral line widths. It has been pointed out, particularly by G. Hettner,[46] that the Lorentz collision damping predominates over other causes of line broadening for infra-red absorption by molecules.

The mathematical treatment of the influence of finite slit width upon the observed absorption was initiated, in 1913, by R. Ladenburg and F. Reiche.[47] D. M. Dennison,[48] in 1928, gave a detailed theoretical discussion of the observed shape and intensity of infra-red absorption lines. Dennison's theory was applied and extended by L. A. Matheson[49] and by C. L. Pekeris.[50] In these investigations, the individual absorption lines were considered to be completely separated from each other. Recently, however, W. M. Elsasser[51] has treated the idealized case of an infinite sequence of equidistant, identical, and partly overlapping absorption lines. His theory has been applied by J. Strong and others.[52–54]

In this section, the theory of Dennison will be extended somewhat and applied, together with Elsasser's theory, to problems of practical infra-red spectroscopy.

Spectrometer Transmission Function

When a spectrometer is set to transmit radiation of a certain frequency ν_i, it will actually transmit a frequency band of finite width. The width of this frequency band will depend upon the widths of the entrance and exit slits, on the diffraction occurring in the aperture of the dispersive system, on the aberrations in the lenses or mirrors, and on the energy distribution in the source of radiation.

If the slits are infinitely narrow and the mirrors or lenses free from aberrations, the energy distribution in the transmitted frequency band will be given by the diffraction function

$$c \sin^2 (\pi(\nu-\nu_i)/\Delta\nu_i)/(\nu-\nu_i)^2,$$

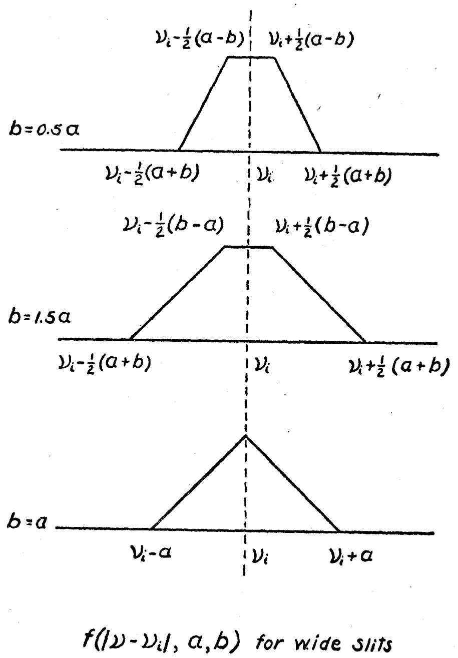

FIG. 5. Spectrometer transmission function for entrance and exit slits so wide that diffraction in prism can be neglected. a is the width of the entrance slit, in frequency units; b the width of the exit slit; ν_i is the frequency for which the spectrometer is set. The form of the transmission function is illustrated for three values of the ratio b/a.

where $\Delta\nu_i=\nu_i/Nn$ for a grating spectrograph (N = number of rulings; n = order of spectrum) and $\Delta\nu_i=\nu_i/B(d\mu/d\lambda)$ for a prism instrument (B = base length of prism; μ = refractive index of prism material). If the secondary maxima are neglected, this function is different from zero only for $\nu_i-\Delta\nu_i<\nu<\nu_i+\Delta\nu_i$.

If the slits are wide, as is usually the case in the infra-red, the diffraction and the aberrations may be neglected. If, in addition, the energy per unit frequency interval of the source S_ν varies but slowly with the frequency, the energy distribution in the transmitted frequency band will have a form such as those shown in Fig. 5. Here a is the width of the entrance slit, and b the width of the exit slit. Since it is common practice to work with slits of equal width, only the triangular energy distribution shown at the bottom will be considered here.

The effect of diffraction and aberrations will be to round off the peak of the energy distribution curve and to spread out its sides somewhat. When these effects are appreciable, the transmission function will resemble a Gaussian error function. Ladenburg and Reiche[47] took the spectrometer transmission function to be constant in the frequency interval ν_i-a, ν_i+a and zero outside this interval. Dennison[48] used a Gaussian function in most of his work. Since the energy distribution is an even function of $\nu-\nu_i$, we shall denote it by $f(|\nu-\nu_i|, a)$. For the purpose of a general survey, the exact form of $f(|\nu-\nu_i|, a)$ is not very important. We shall in most cases use the "triangular" form; i.e.,

$$f(|\nu-\nu_i|,a)=\begin{cases}0 & \text{when } \nu\leqq\nu_i-a\\ (\nu-\nu_i+a)f(0,a)/a & \text{when } \nu_i-a\leqq\nu\leqq\nu_i\\ (\nu_i+a-\nu)f(0,a)/a & \text{when } \nu_i\leqq\nu\leqq\nu_i+a\\ 0 & \text{when } \nu\geqq\nu_i+a.\end{cases} \tag{3}$$

Obviously,

$$\int_0^\infty f(|\nu-\nu_i|,a)d\nu_i=\int_0^\infty f(|\nu-\nu_i|,a)d\nu=\int_{\nu_i-a}^{\nu_i+a} f(|\nu-\nu_i|,a)d\nu=af(0,a). \tag{4}$$

Transmittance

Let an absorption cell of length l filled with a gas having the absorption coefficient k_ν for radiation of the frequency ν be placed in the path of the radiation in front of the entrance slit of the spectrometer. The observed transmittance T_i at the frequency setting ν_i is then defined by I_i/I_{0i}, where I_{0i} is the intensity of the radiation transmitted by cell and spectrometer when the cell is empty, and I_i the intensity of the radiation transmitted when the cell is filled with the absorbing gas. If S_ν represents the energy distribution in the radiation reaching the slit through the empty cell, T_i is given by the expression

$$T_i=I_i/I_{0i}=\int_0^\infty S_\nu \exp(-k_\nu l)f(|\nu-\nu_i|,a)d\nu \bigg/ \int_0^\infty S_\nu f(|\nu-\nu_i|,a)d\nu. \tag{5}$$

Usually, the frequency interval transmitted by the spectrometer is so narrow that S_ν may be regarded as constant over this interval. Equation (5) then takes the simpler form

$$T_i=\int_0^\infty \exp(-k_\nu l)f(|\nu-\nu_i|,a)d\nu \bigg/ \int_0^\infty f(|\nu-\nu_i|,a)d\nu. \tag{6}$$

If the triangular form (3) is used for the function $f(|\nu-\nu_i|, a)$, the limits of the integrals may be changed to ν_i-a and ν_i+a, and the integral in the denominator reduces to $af(0, a)$.

There are certain cases in which the observed transmittance is independent of the slit width a of the spectrometer. One case is that of an absorption coefficient which is independent of frequency. Another case, considered by Elsasser,[51] is that of an absorption band consisting of a large number of equally spaced identical absorption lines of which very many lie in the frequency range in which $f(|\nu-\nu_i|, a)$ is different from zero. The absorption coefficient k_ν will in this case be periodic with a period d which is so small that $f(|\nu-\nu_i|, a)$ does not change appreciably over the range d. The integral in the numerator of (6)

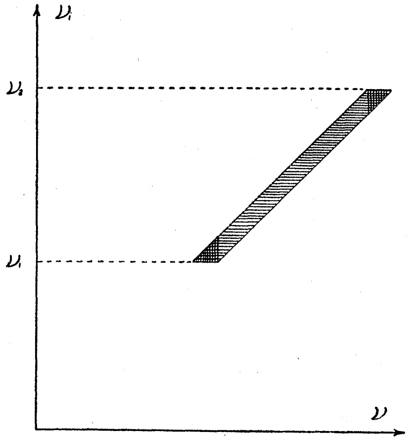

FIG. 6. Range over which double integration is to be carried out.

may then be written

$$\sum_{n=1}^{\infty}\int_{nd}^{(n+1)d}\exp(-k_\nu l)f(|\nu-\nu_i|,a)d\nu$$

$$=\sum_{n=1}^{\infty}f(|(n+\tfrac{1}{2})d-\nu_i|,a)\cdot\int_{nd}^{(n+1)d}\exp(-k_\nu l)d\nu$$

$$=\int_{\nu_i}^{\nu_i+d}\exp(-k_\nu l)d\nu\cdot\sum_{n=1}^{\infty}f(|(n+\tfrac{1}{2})d-\nu_i|,a).$$

The denominator can be written

$$\sum_{n=1}^{\infty}\int_{nd}^{(n+1)d}f(|\nu-\nu_i|,a)d\nu$$

$$=d\cdot\sum_{n=1}^{\infty}f(|(n+\tfrac{1}{2})d-\nu_i|,a).$$

Thus, the transmittance becomes

$$T=\frac{1}{d}\int_{\nu}^{\nu+d}\exp(-k_\nu l)d\nu. \tag{7}$$

The subscript i has been omitted since the value of the transmittance is independent of the setting of the spectrometer as long as ν_i lies well within the absorption band.

A third case in which the transmittance is independent of the slit width is that of numerous, randomly distributed, absorption lines lying in the frequency range transmitted by the spectrometer. A simple consideration shows that in this case the transmittance is given approximately by the expression

$$T=\frac{1}{\nu_2-\nu_1}\int_{\nu_1}^{\nu_2}\exp(-k_\nu l)d\nu. \tag{8}$$

The limits ν_1 and ν_2 are arbitrary except that the interval $\nu_2-\nu_1$ must contain a large number of absorption lines, and ν_1 and ν_2 must lie well within the band.

Integrated Transmittance

When a single absorption line is studied with a spectrometer of high dispersion, the transmittance T_i is usually measured or recorded over a range of frequencies ν_i covering the line, and the integral of T_i over the line is evaluated. Under certain conditions, the integral,

$$J=\int_{\nu_1}^{\nu_2}T_i d\nu_i, \tag{9}$$

becomes practically independent of the slit width a. Assume first that the limits ν_1 and ν_2 are so close together that $S_{\nu 1}$ and $S_{\nu 2}$ can be regarded as equal but that at the same time $\nu_2-\nu_1\gg a$. Then (6) can be used for T_i, and if the form (3) is used for $f(|\nu-\nu_i|,a)$,

$$J=\frac{1}{af(0,a)}\int_{\nu_1}^{\nu_2}\int_{\nu_i-a}^{\nu_i+a}\exp(-k_\nu l)f(|\nu-\nu_i|,a)d\nu d\nu_i.$$

The double integral is to be evaluated over the range of values of ν and ν_i lying in the shaded area shown in Fig. 6. Interchanging the order of integration,

$$J=\frac{1}{af(0,a)}\int_{\nu_i-a}^{\nu_i+a}\exp(-k_\nu l)\left(\int_{\nu_1}^{\nu_2}f(|\nu-\nu_i|,a)d\nu_i\right)d\nu.$$

The integral in the parenthesis is equal to $af(0, a)$ when $\nu_1+a\leqq\nu\leqq\nu_2-a$; hence,

$$J=\int_{\nu_1+a}^{\nu_2-a}\exp(-k_\nu l)d\nu+\frac{1}{af(0,a)}\cdot\left\{\int_{\nu_1-a}^{\nu_1+a}\exp(-k_\nu l)\left(\int_{\nu_1}^{\nu_2}f(|\nu-\nu_i|,a)d\nu_i\right)d\nu\right.$$

$$\left.+\int_{\nu_2-a}^{\nu_2+a}\exp(-k_\nu l)\left(\int_{\nu_1}^{\nu_2}f(|\nu-\nu_i|,a)d\nu_i\right)d\nu\right\}.$$

Since the integration with respect to ν_i is assumed to cover essentially the entire absorption line, k_ν will be very small, and $\exp(-k_\nu l)\cong 1$ when $\nu_2-a\leqq\nu\leqq\nu_2+a$, and when $\nu_1-a\leqq\nu\leqq\nu_1+a$. Consequently,

$$J=\int_{\nu_1+a}^{\nu_2-a}\exp(-k_\nu l)d\nu+\frac{1}{af(0,a)}\left\{\int_{\nu_1-a}^{\nu_1+a}\int_{\nu_1}^{\nu_2}f(|\nu-\nu_i|,a)d\nu_i d\nu+\int_{\nu_2-a}^{\nu_2+a}\int_{\nu_1}^{\nu_2}f(|\nu-\nu_i|,a)d\nu_i d\nu\right\}.$$

The sum of the two double integrals, which extend over the doubly shaded areas in Fig. 6, is

$$\int_{\nu_1-a}^{\nu_1+3a}\int_{\nu_1}^{\nu_1+2a}f(|\nu-\nu_i|,a)d\nu_i d\nu=2a^2f(0,a).$$

Hence

$$J=\int_{\nu_1+}^{\nu_2-a}\exp(-k_\nu l)d\nu+2a,$$

which may be written as

$$J=\int_{\nu_1}^{\nu_2}\exp(-k_\nu l)d\nu, \tag{10}$$

since $\exp(-k_\nu l)\cong 1$ close to the limits of integration.

Thus under the condition specified, the so-called "total absorption" is given by

$$A=\int_{\nu_1}^{\nu_2}(1-T_i)d\nu_i=\int_{\nu_1}^{\nu_2}(1-\exp(-k_\nu l))d\nu. \tag{11}$$

This formula has been used by Dennison and others without proof. It is clear that the derivation given here does not depend essentially upon the use of the triangular distribution function (3).

Absorption Coefficient When Line Broadening is Caused by Collision Damping

When the line broadening is caused by collision damping, the absorption coefficient is given by a general expression of the form[44, 45]

$$k_\nu=\sum_m k_{\nu m}=\sum_m(\alpha_m\delta/\pi[(\nu-\nu_m)^2+\delta^2]). \tag{12}$$

Each term in the sum represents a single absorption line. Each line is characterized by two constants: the frequency ν_m of the center of the line and the constant $\alpha_m=\int_0^\infty k_{\nu m}d\nu$ which is proportional to the so-called "oscillator strength" of the line. The damping constant δ, which determines the line width, is common to all the lines. Under normal conditions, δ is given approximately by the following expression[44, 45]

$$\delta=\pi^{-1}n(2\pi kT)^{\frac{1}{2}}\rho^2\left(\frac{m+M}{mM}\right)^{\frac{1}{2}}, \tag{13}$$

where n is the number of molecules per unit volume, k Boltzmann's constant, T the absolute temperature, ρ the "optical collision radius," m the mass of the absorbing molecule, and M the mass of the foreign molecules.

The validity and accuracy of these formulas need not be discussed here. For our purpose the following facts are essential. If no quenching occurs, the constants α_m are proportional to the concentration of the absorbing gas and, hence, very nearly proportional to its partial pressure p. On the other hand, δ is proportional to the total number of molecules per unit volume and, hence, to the total pressure, P.

Continuous Absorption

The transmittance will now be evaluated for three limiting cases. First, assume that k_ν varies so slowly with frequency as to be practically constant over the frequency range transmitted by the spectrometer. This will be the case when the instrument is set for a frequency ν_i sufficiently far from any region in which line centers occur. That the absorption coefficient may well be appreciably different from zero for such a frequency has been pointed out by Elsasser.[55]

If the thickness l of the absorbing gas is not too great, the factor exp $(-k_\nu l)$ will be practically constant, say equal to exp $(-k_0 l)$, over the frequency interval ν_i-a, ν_i+a transmitted by the spectrometer, and this factor may be taken outside the integral sign in the numerator of (5). The expression then reduces to

$$T=\exp(-k_0 l). \tag{14}$$

The subscript has been omitted since the transmittance is independent of frequency over a more or less wide range.

If the *extinction* be defined as $E=-\ln T$,* (14) gives $E=k_0 l$. Thus, the extinction is proportional to the cell length l; i.e., Lambert's law holds. Also, since the absorption constant k_0 will be proportional to the concentration of the absorbing gas, Beer's law holds in this case. If the absorbing gas may be regarded as ideal, the extinction will be proportional to the partial pressure p. If the frequency ν_i is not too far outside an extended region containing numerous centers of absorption lines, the absorption coefficient k_0 and, hence, the extinction E will be independent of the total pressure P.

If the frequency ν_i for which the spectrometer is set is too close to line centers for the conditions assumed here to hold with great accuracy, k_ν may still be a slowly varying function of frequency. In that case, the correction methods developed by F. Paschen[56] and by C. Eckart[57] may be used to determine the transmittance with a considerable degree of accuracy.

Single Absorption Line

The case of a single isolated absorption line will be considered next. The absorption coefficient is assumed to consist of only one term, and the observed transmittance at ν_i is given by the expression

$$T_i=\int_0^\infty \exp\left[-\frac{\pi^{-1}\alpha\delta l}{(\nu-\nu_m)^2+\delta^2}\right]f(|\nu-\nu_i|,a)d\nu\Big/\int_0^\infty f(|\nu-\nu_i|,a)d\nu. \tag{15}$$

The integral in the numerator can be integrated in terms of known functions neither for the triangular form (3) for $f(|\nu-\nu_i|, a)$ used here nor for the Gaussian error function used by Dennison. For the practical spectroscopist, the minimum transmittance T_m obtained when the spectrometer is set at the center of the absorption line is of greatest interest. Substitution of ν_m for ν_i in (15) gives

$$T_m=\int_0^\infty \exp\left[-\frac{\pi^{-1}\alpha\delta l}{(\nu-\nu_m)^2+\delta^2}\right]f(|\nu-\nu_m|,a)d\nu\Big/\int_0^\infty f(|\nu-\nu_m|,a)d\nu. \tag{16}$$

This expression, as well as (15), can be evaluated only by approximation methods. The most obvious procedure is to expand the exponential function and integrate term for term. When the

---

* In practical spectroscopy, the extinction is usually defined as $-\log_{10} T=-0.4343 \ln T$.

triangular form (3) is used for $f(|\nu-\nu_m|, a)$, this leads to the expression

$$T_m=1-\frac{s}{1!}\left(2\tan^{-1}\frac{1}{r}-r\ln\frac{1+r^2}{r^2}\right)+\frac{s^2}{2!}\frac{1}{r}\tan^{-1}\frac{1}{r}-\frac{s^3}{3!}\left(\frac{1}{4r(1+r^2)}+\frac{3}{4r^2}\tan^{-1}\frac{1}{r}\right)+\cdots$$
$$+\frac{(-s)^n}{n!}\left\{-\frac{(1+r^2)^{n-2}-r^{2n-4}}{(n-1)r^{n-2}(1+r^2)^{n-2}}+\sum_{j=2}^{n-1}\frac{(2n-3)(2n-5)\cdots(2n-2j+1)r^{n-2j}}{2^{j-1}(n-1)(n-2)\cdots(n-j)(1+r^2)^{n-j}}\right.$$
$$\left.+\frac{(2n-3)(2n-5)\cdots 3.1}{2^{n-2}(n-1)!r^{n-3}}\cdot\tan^{-1}\frac{1}{r}\right\}+\cdots, \quad (17)$$

where $r=\delta/a$ and $s=\alpha l/\pi a$.

This expression converges for all values of r and s, but the convergence is not very rapid except when s is small and r not too small.

When the form (3) is used for $f(|\nu-\nu_m|, a)$, the integral in the numerator of (16) can be separated into two integrals, one of which can be readily evaluated. If r is small compared to one, the other integral can be expressed approximately in terms of known functions by means of certain formulas derived by Ladenburg and Reiche.[47] The resulting expression for T_m, holding for $r\ll 1$, is

$$T_m=2e^{-rs}-(1+r^2)\exp\left[-\frac{rs}{1+r^2}\right]+r\exp\left[-s/r\right]+\pi s\exp\left[-s/2r\right]\left[J_0\left(i\frac{s}{2r}\right)-J_1\left(i\frac{s}{2r}\right)\right]$$
$$+2(\pi rs)^{\frac{1}{2}}\Phi(r^{\frac{1}{2}}s^{\frac{1}{2}})+rsEi\left(-\frac{s}{r}\right)-rsEi\left(-\frac{rs}{1+r^2}\right). \quad (18)$$

Here J_0 and J_1 are Bessel functions of zeroth and first order, respectively; Φ is the probability integral and Ei the exponential integral.

Dennison[48] has given a somewhat similar formula. Using the triangular form for $f(|\nu-\nu_m|, a)$ and dropping δ^2 in the denominator of the exponent in (16), which is permitted when $r\ll s$, he found (our notations)

$$T_m=e^{-rs}-2(\pi rs)^{\frac{1}{2}}(1-\Phi(r^{\frac{1}{2}}s^{\frac{1}{2}}))+rs(\ln(rs)-0.5772)+(rs)^2-\frac{1}{2\cdot 2!}(rs)^3+\frac{1}{3\cdot 3!}(rs)^4-\cdots. \quad (19)$$

If $r\ll 1$, $r\ll s$ and $rs<1$, (18) and (19) may be expanded. If only the first two terms are retained, both formulas give

$$T_m=1-2(\pi rs)^{\frac{1}{2}}+\cdots=1-2\frac{(\alpha l\delta)^{\frac{1}{2}}}{a}+\cdots, \quad (20)$$

and hence for the maximum extinction,

$$E_m=-\ln T_m=2(\alpha l\delta)^{\frac{1}{2}}/a. \quad (21)$$

When δ^2 is dropped in the denominator of the expression for the absorption coefficient, the use of a Gaussian error function for $f(|\nu-\nu_m|, a)$ is more convenient than the triangular form (3), since the integrals in numerator and denominator of (16) can then be readily evaluated. Taking $f(|\nu-\nu_m|, a)=\exp\left[-2.77(\nu-\nu_m)^2/a^2\right]$, where the numerical constant is chosen so as to make the half-value width the same as for the triangular form, Dennison[48] found (our notations)

$$\begin{aligned}T_m&=\exp\left[-1.879(\pi rs)^{\frac{1}{2}}\right]\\&=\exp\left[-1.879(\alpha l\delta)^{\frac{1}{2}}/a\right],\end{aligned} \quad (22)$$

$$E_m=1.879(\alpha l\delta)^{\frac{1}{2}}/a. \quad (23)$$

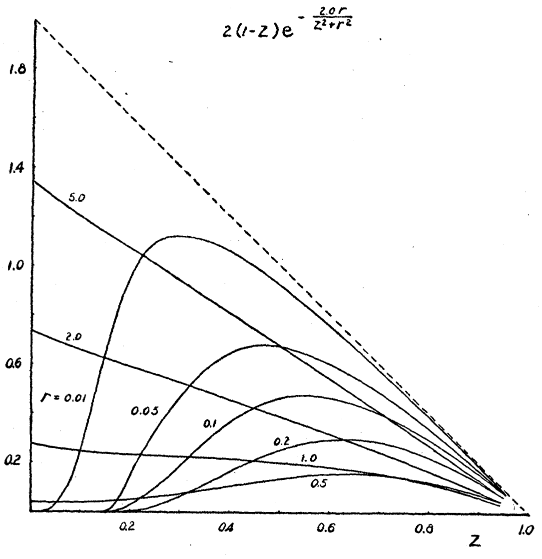

FIG. 7. Plots of the function $2(1-z)\exp(-2.0r/(r^2+z^2))$ for $r=\delta/a=0.01$, 0.05, 0.1, 0.2, 0.5, 1.0, 2.0, or 5.0.

Formulas (21) and (23) are identical except for a difference of about 6 percent in the value of the numerical factor. It is clear that the triangular form of $f(|\nu-\nu_m|, a)$ should give a greater value for the maximum extinction than the Gaussian form. Which of the two formulas, (21) or (23), is the more correct will depend upon the experimental circumstances. At the longest wavelengths, where wide slits must be used, (21) is generally more correct; whereas at short wavelengths, (23) will usually be the more appropriate formula.

Equation (23) has been used successfully to account for measurements on individual strong absorption lines. The formula predicts that the extinction is proportional to the square root of the cell length and, for constant product of cell length and partial pressure, to the square root of the total pressure.

Dennison[48] has given two expressions for the "total absorption" A. One is an approximation formula obtained by dropping δ^2 in the denominator of the absorption coefficient; the other is a series expansion. Since the quantity A has hardly yet found use in chemical spectroscopy, these formulas will not be discussed here.

Since each of the formulas (17)–(23) is applicable or valid only over a limited range of the parameters, these formulas are not very useful in providing an over-all picture of the manner in which T_m depends on the parameters $r=\delta/a$ and $s=\alpha l/\pi a$. To obtain such a picture we have resorted to numerical integration of the general expression (16) for T_m.

When the triangular form (3) of $f(|\nu-\nu_m|, a)$ is substituted in (16), this formula is readily reduced to

$$T_m=\int_0^1 2(1-z)\exp(-rs/(r^2+z^2))dz. \quad (24)$$

In Fig. 7 the integrand in (24) has been plotted for $s=2.0$ and eight different values of r. Similar curves obtained for $s=0.2$ are shown in Fig. 8.

The minimum transmittance T_m corresponding to given values of r and s was determined by measuring the area under the proper curve by means of a planimeter. Taking the negative logarithm of the values obtained for T_m, we get the corresponding maximum (practical) extinction values, $E_m=-\log T_m$. In Fig. 9 the values of E_m thus obtained have been plotted against r. For small values of r, the maximum extinction increases rapidly with increasing r; then E_m reaches a maximum and falls off slowly as r is increased further. The smaller s is (i.e., the weaker the absorption line or the shorter the cell length) the smaller is the value of r at which the maximum occurs. Since δ and, hence, $r=\delta/a$ are pro-

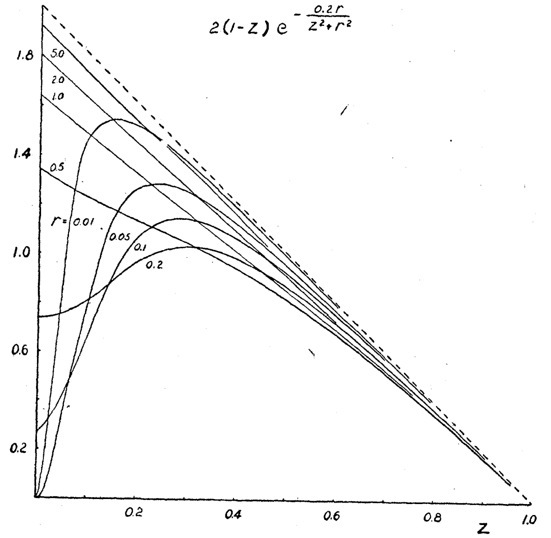

FIG. 8. Plots of the function $2(1-z)\exp(-0.2r/(r^2+z^2))$ for $r=\delta/a=0.01$, 0.05, 0.1, 0.2, 0.5, 1.0, 2.0, or 5.0.

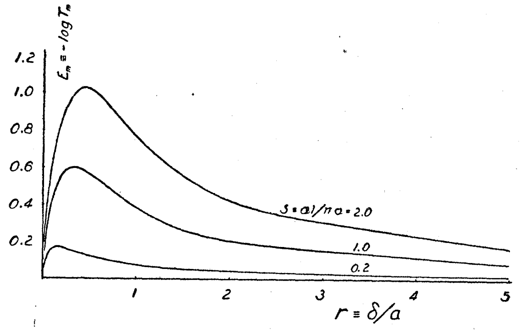

FIG. 9. Maximum extinction, $E_m = -\log T_m$, at center of single absorption line plotted against the parameter $r = \delta/a$ for $s = \alpha l/\pi a = 0.2$, 1.0, or 2.0. Illustrates variation of maximum extinction with total pressure for constant product of partial pressure and cell length.

portional to the total pressure, whereas $s = \alpha l/\pi a$ is proportional to the product of the partial pressure and the cell length, the curves shown in Fig. 9 illustrate the variation of the maximum extinction E_m with total pressure when the product of the partial pressure and the cell length is kept constant.

In Fig. 10 the values of the maximum extinction E_m in an isolated absorption line corresponding to a constant value of r have been plotted against the parameter s. Since α, and therefore $s = \alpha l/\pi a$, is proportional to the concentration of the absorbing gas, while δ, and therefore $r = \delta/a$, is proportional to the total pressure P, these curves may be regarded as "working curves" for total constant pressure of the mixture containing the absorbing gas. Since s is proportional to the cell length, these curves also show how the maximum extinction varies with the cell length at constant pressure. When r is sufficiently large, i.e., when the total pressure P is sufficiently high, these curves are straight.

When the absorbing gas is pure, i.e., not mixed with any foreign gas, the total pressure P is equal to the partial pressure p. Since r is proportional to the total pressure and s is proportional to the partial pressure, they must be proportional to each other in this case, i.e., r/s must be a constant. In Fig. 11, the maximum extinction E_m for a single absorption line has been plotted against r for various constant values of r/s. For large values of r/s, i.e., for low values of the oscillator strength, the extinction reaches a flat maximum for a certain value of r and then falls off slightly. On the other hand, for small values of r/s, i.e., for high intensities of the absorbing line, the extinction is proportional to r, and hence to the pressure, over the range considered.

The curves shown in Fig. 11 also illustrate the variation of maximum extinction with slit width for a single absorption line. If the slit width a is increased for constant values of α, δ, and l, the parameters $r = \delta/a$ and $s = \alpha l/\pi a$ are both decreased in the same ratio, so that r/s remains constant. Thus, since the abscissa is $r = \delta/a$, these curves give the maximum extinction E_m as a function of the reciprocal of the slit width for various values of $r/s = \pi\delta/\alpha l$. For large values of $\pi\delta/\alpha l$ and small values of a, E_m is practically independent of the slit width. On the other hand, for small values of $\pi\delta/\alpha l$, E_m is inversely proportional to the slit width. If E_m had been plotted against a, the curves would in this case be right hyperbolas.

The case of a single isolated absorption line is a very special case in molecular spectra. Even when it is approximated closely, there will usually be some additional absorption caused by absorption lines having their centers outside the frequency band transmitted by the spectrometer. As a result, there will be added to the absorption coefficient k_ν considered above a term k_0 which is independent of the frequency within the narrow frequency band transmitted by the spectrometer. Thus, the transmittance T_m which we have computed should be multiplied by a factor $\exp[-k_0 l]$ and, hence, there should be added a term $0.4343k_0 l$ to the extinction. This additional extinction is proportional to the concentration of

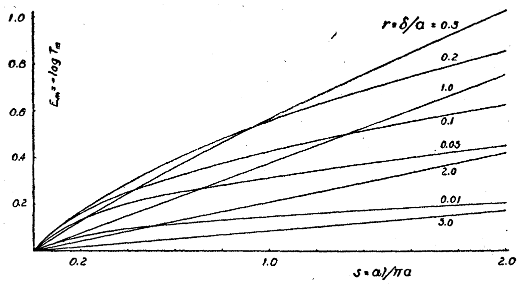

FIG. 10. Maximum extinction at center of single absorption line as function of the parameter $s = \alpha l/\pi a$ for $r = \delta/a = 0.01$, 0.05, 0.1, 0.2, 0.5, 1.0, 2.0, or 5.0. Illustrates working curves for total constant pressure as well as dependence on cell length at constant pressure.

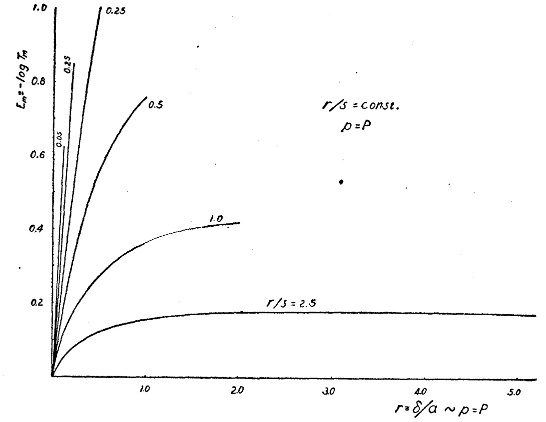

FIG. 11. Maximum extinction at center of single absorption line as a function of $r=\delta/a$ when $r/s=\pi\delta/\alpha l$ is kept constant. Illustrates variation of extinction with pressure when absorbing gas is pure. Also shows maximum extinction as a function of the reciprocal of the slit width.

the absorbing gas, but will usually be independent of the total pressure and the slit width. It will tend to straighten out the working curves.

Numerous Equidistant Identical Absorption Lines

In infra-red bands of polyatomic molecules, the individual lines generally lie so close together that a considerable number of them have their centers in the narrow frequency range transmitted by the spectrometer. The idealized case of an absorption band consisting of an infinite sequence of equidistant identical absorption lines, of which many fall in the frequency band transmitted by the spectrometer, has been treated by W. M. Elsasser.[51] Using Eq. (7) and the following expression for the absorption coefficient

$$k_\nu = \sum_{n=-\infty}^{n=+\infty} \frac{\pi^{-1}\alpha\delta}{(\nu-nd)^2+\delta^2}, \tag{25}$$

where d is the distance, in frequency units, between neighboring line centers, Elsasser obtained the following general formula for the transmittance

$$T=\int_{st}^{\infty} \exp\left[-v \coth 2rt\right]\cdot J_0\left(i\frac{v}{\sinh 2rt}\right)dv. \tag{26}$$

Here we have, for convenience, introduced the previously used symbols $r=\delta/a$ and $s=\alpha l/\pi a$. The new symbol t is defined as $\pi a/d$. J_0 is the Bessel function of zeroth order. Of course, since only the products st and rt occur in (26), the transmittance T and hence the extinction E are independent of the slit width a.

For small values of $rt=\pi\delta/d$ the expression (26) reduces to

$$T=1-\Phi(r^{\frac{1}{2}}s^{\frac{1}{2}}t)=1-\Phi\left(\frac{(\pi\alpha l\delta)^{\frac{1}{2}}}{d}\right), \tag{27}$$

where Φ is the probability integral. For large values of rt, Elsasser obtained the approximation formula

$$T=\exp\left[-st \tanh 2rt\right]\cdot J_0\left(i\frac{st \tanh 2rt}{\cosh 2rt}\right). \tag{28}$$

Taking t equal to 10, we have computed the transmittance for three values of s and eight values of r, using the two special formulas (27) and (28) and adjusting the curves to join smoothly. Figure 12 shows the values for the extinction, $E=-\log T$, derived from the transmittance values obtained in this manner. For a given value of s, the extinction increases rapidly at first and then slowly with r until it reaches a constant value. This occurs for a smaller value of r the smaller s is. Since r is proportional to the total pressure and s is proportional to the product of the partial pressure and the cell length, these curves illustrate the dependence of the extinction

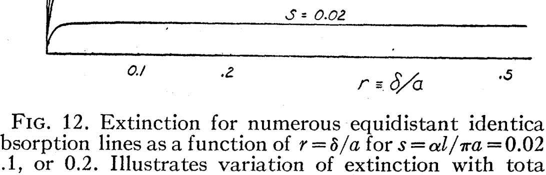

FIG. 12. Extinction for numerous equidistant identical absorption lines as a function of $r=\delta/a$ for $s=\alpha l/\pi a=0.02$, 0.1, or 0.2. Illustrates variation of extinction with total pressure for constant product of partial pressure and cell length.

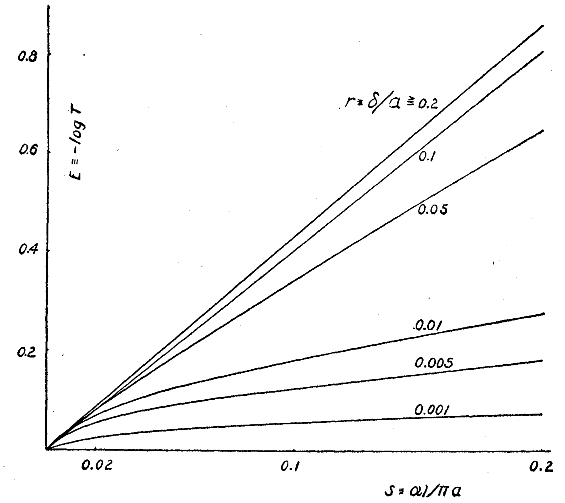

FIG. 13. Extinction for numerous equidistant identical absorption lines as function of $s=\alpha l/\pi a$ for $r=0.001$, 0.005, 0.01, 0.05, 0.1 or $r\geqq 0.2$. Illustrates working curves for constant total pressure as well as dependence upon cell length at constant pressure.

upon the total pressure for constant product of partial pressure and cell length. The curves resemble closely some of the experimental curves obtained by v. Bahr and others.

In Fig. 13, we have plotted the extinction against s for various constant values of r. These curves may be regarded as working curves for the absorbing gas in mixtures of constant total pressure. When the total pressure is sufficiently high, they are straight lines and independent of the total pressure. These curves also represent the extinction as a function of the cell length.

To show the manner in which the extinction varies with pressure when no foreign gas is mixed with the absorbing gas, the values of the extinction E corresponding to constant values of r/s have been plotted against r in Fig. 14. The curves are straight and independent of r/s for large values of this ratio. They are slightly convex to the horizontal axis for small values of r/s.

EXPERIMENTAL EXAMPLES

The idealized cases considered in the preceding sections, namely, an absorption independent of the frequency, a single isolated absorption line, and an infinite sequence of identical equidistant lines, represent different extremes between which the absorption by actual gases may be expected to fall. A careful experimental study of the absorption laws for different types of infra-red bands of a variety of molecules would be desirable, but very laborious. The greatest difficulty in such work is that of correcting with sufficient precision for stray light in the spectrometer. If this correction is not estimated accurately, the working curves will be distorted. Although the stray radiation for a given wave-length setting does not vary greatly when the cell is filled with different mixtures of similar gases, such as the lower paraffin hydrocarbons, the dependence of the stray radiation upon the composition of the gas mixture cannot always be neglected. Unfortunately, there is no simple way of determining the stray radiation, and double monochrometers are not yet available for infra-red work. For readily condensible gases, such as the C_4 hydrocarbons, the deviations from the simple gas laws must be taken into consideration when the transmittance curves are plotted.

Although we have not made a systematic study of the absorption laws for gases in the infra-red, we have made careful observations on selected absorption bands of a number of gaseous hydrocarbons. The spectrometer used in all of this work is a Littrow type instrument with a rocksalt prism of face 80×100 mm and an on-axis parabolic mirror of focal length 91.4 cm. We shall present here a few typical results obtained with C_4 hydrocarbons.

Figure 15 shows the extinction at 8.47μ of mixtures of a constant amount of isobutane and

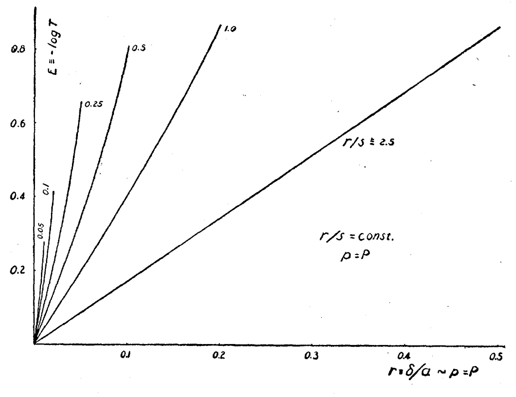

FIG. 14. Extinction for numerous equidistant identical absorption lines as function of $r=\delta/a$ when $r/s=\pi\delta/\alpha l$ is kept constant. Illustrates variation of extinction with pressure when absorbing gas is pure.

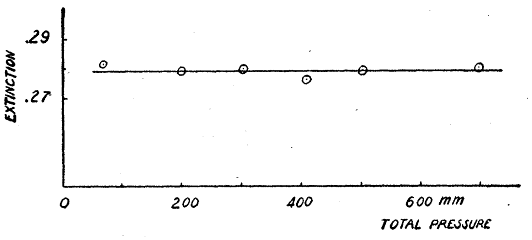

FIG. 15. Extinction at 8.47μ of a constant amount of isobutane mixed with different amounts of nitrogen. Partial pressure isobutane: 68.3 mm cell: 9.75 cm slits: 0.46 mm.

different amounts of nitrogen. The partial pressure of the isobutane was 68.3 mm of mercury; the cell length was 9.75 cm; and the width of the entrance and exit slits of the spectrometer was 0.46 mm. The temperature of the gas varied a few tenths of a degree around 28.4°C. Within the experimental error, the extinction is independent of the total pressure, showing that in the pressure range used the addition of nitrogen has no influence upon the absorption of isobutane at 8.47μ.

In Fig. 16, the results of two sets of measurements have been superposed. The squares represent extinction values obtained at 6.26μ with different amounts of pure butadiene-1, 3 in the cell, and the circles represent extinctions obtained with different amounts of butadiene in nitrogen at a constant total pressure of 700 mm. The cell length in this case was 5.4 cm, the slit width 0.20 mm, and the temperature 27.8°C. The extinctions are plotted against the partial pressure of butadiene. The two sets of points lie very nearly on the same curve which is only slightly curved. The wave-length 6.26μ is often used for analysis.

Figure 17 shows two sets of similar experimental data for butadiene obtained with the spectrometer set at the center of the *Q*-branch of the 11.0μ band. The cell length was 9.75 cm; the slit width 1.00 mm. The squares represent extinction values obtained when the cell was filled with pure butadiene. These measurements were made on two successive days, the temperature of the gas being 24.6°C on one day and 28.2°C the next. The circles represent data for different amounts of butadiene in nitrogen at a constant total pressure of 700 mm. The temperature of the gas was 28.2°C. The circles lie slightly above a curve drawn through the squares, indicating that the presence of nitrogen slightly enhances the extinction of butadiene at 11.0μ. We have established the reality of this effect, using much smaller partial pressures of butadiene. Thus, when nitrogen is added to 1 mm of butadiene in a 43 cm cell until the total pressure reaches 130 mm, the extinction at 11.0μ increases about 5 percent. For the other bands of butadiene and for most bands of the other C_4 hydrocarbons, the variation of the extinction with the total pressure is so small that it can be detected only with difficulty, if at all.

The case of butadiene at 11.0μ approaches that of a single absorption line on a uniform background. It will be noticed that the curvature of the curve in Fig. 17 is very great.

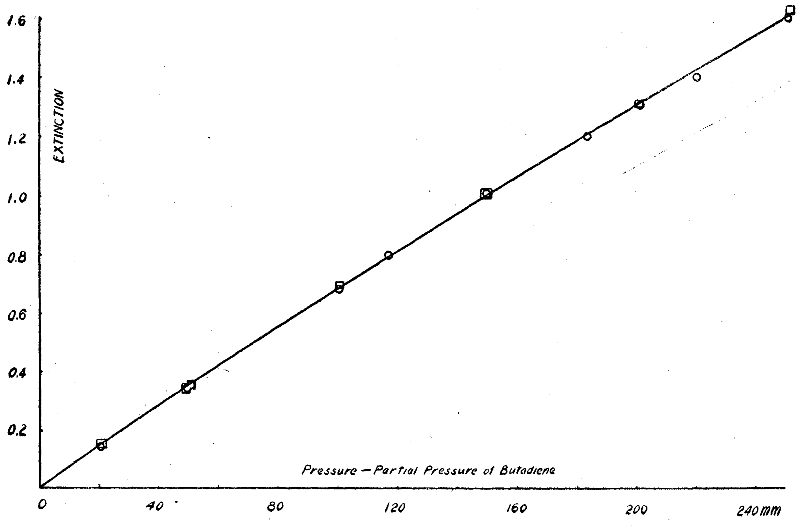

FIG. 16. Extinction at 6.26μ of butadiene (squares) and of butadiene in nitrogen (circles). Total pressure: 700 mm; cell: 5.4 cm; slits: 0.20 mm.

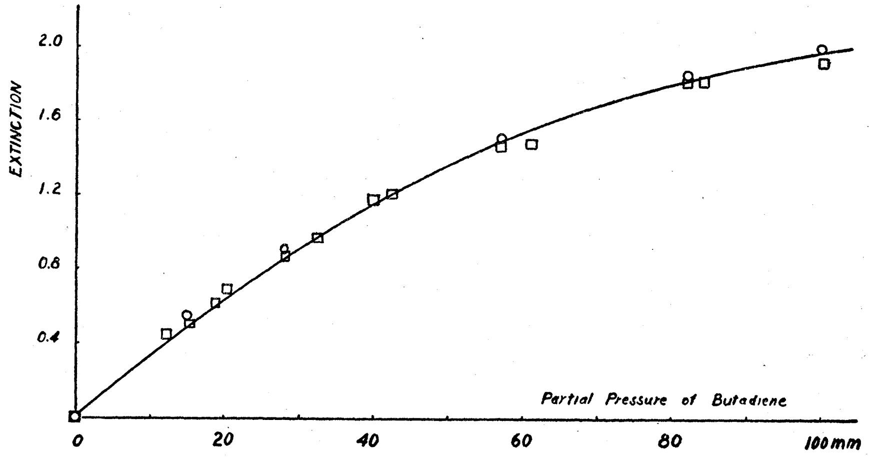

FIG. 17. Extinction at 11.0μ of butadiene squares) and of butadiene in nitrogen (circles). Total pressure 700 mm; cell: 9.75 cm; slit: 1.00 mm.

In Fig. 18 the extinctions of pure isobutene in a 2.00 cm cell at the center of the Q-branch of the 11.23μ band, and slightly off the center, are plotted against the pressure. The curvature is great at both wave-lengths. On the other hand, when the spectrometer is set on the flat maxima of either of the side branches of the 11.23μ isobutene band, a practically straight line is obtained, as shown in Fig. 19.

The last three figures show typical cases of the variation of the measured extinction with slit width. Figure 20 was obtained with the spectrometer set on the Q-branch of the 11.0μ band of butadiene. This is an approach to the case of a single absorption line. The curve resembles a right hyperbola in accord with Eq. (21). In Fig. 21, the spectrometer setting was in what we may call, using a loose terminology, the R-branch of the 11.0μ band of butadiene. The extinction is seen to be nearly independent of the slit width, as it should be in the case of many equidistant absorption lines, as well as in the case of continuous absorption varying slowly with the frequency.

Figure 22 shows the variation of the extinction with slit width for three different wave-lengths in the double band of butadiene at 6.26μ. When the

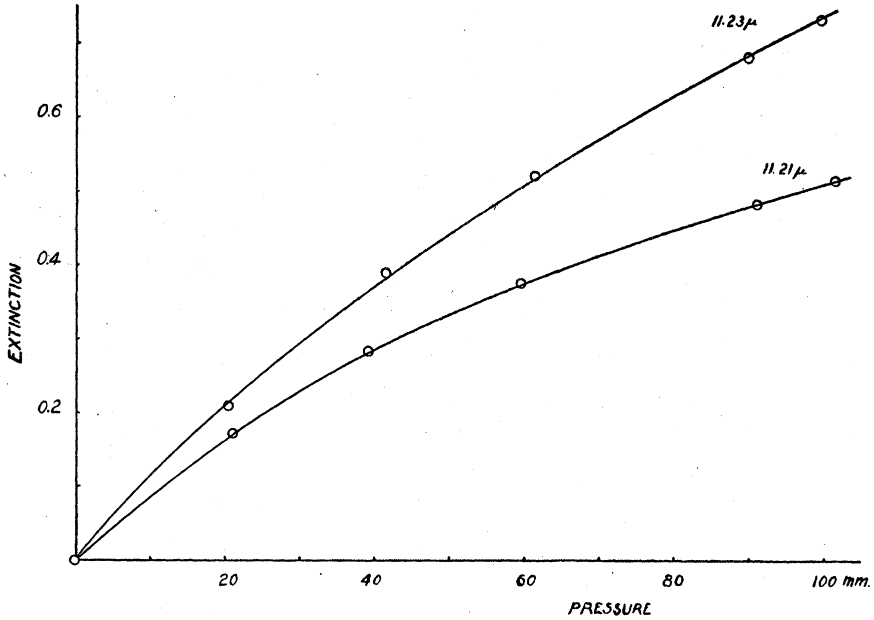

FIG. 18. Extinction of isobutene at 11.23μ (center of Q-branch) and slightly off center. Cell: 2.00 cm; slits: 1.00 mm.

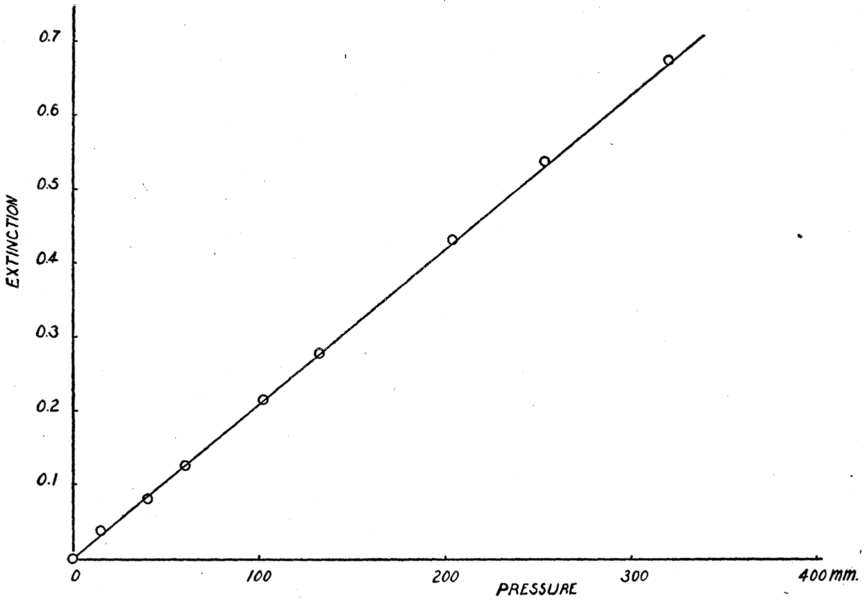

FIG. 19. Extinction of isobutene at 11.44 ("P-branch"). Cell: 2.00 cm; slits: 1.00 mm; center at 11.23μ.

spectrometer is set on either one of the rather sharp absorption maxima at 6.22 and 6.29μ, the observed extinction falls off as the slit width is increased. On the other hand when the spectrometer is set on the fairly sharp absorption minimum at 6.26μ, the measured extinction increases with increasing slit width.

CONCLUDING REMARKS

As indicated by the examples given in the previous section, the theory, in spite of the idealized nature of the cases treated in detail, provides a general explanation of the observed absorption laws for gases in the infra-red. It is to be hoped that more cases will be treated mathematically. However, because of the great labor involved in the theoretical determination of the absorption laws, the information required by the practical spectroscopist must largely be obtained empirically. Although the extinction coefficients needed for accurate quantitative analysis must generally be determined with the spectrometer used, data obtained with other instruments are often very valuable.

If the structure of a band is known from work with a spectrometer of high resolution and if the transmission function $f(|\nu-\nu_i|, a)$ has been determined for a spectrometer of low resolution, it is possible, as we have seen, to compute the shape of the working curves obtained and the dependence of the extinction upon slit width when the latter instrument is used. With some experience it is possible, even without computation, to estimate these data well enough to choose the most favorable wave-lengths for a given analytical problem. As may be seen from a comparison of the working curves given in Figs. 18 and 19, the centers of the strong Q-branches, which are so valuable in qualitative analysis and in the

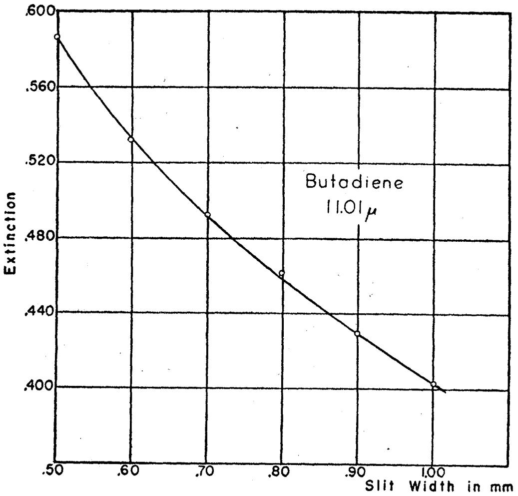

FIG. 20. Variation with slit width of the extinction of butadiene at 11.01μ (center of Q-branch).

determination of traces of compounds, are not always the most desirable wave-lengths when a considerable amount of a compound is to be determined quantitatively. Since the accumulation of all the information needed for analytical applications of infra-red spectroscopy is a laborious task, it is to be hoped that workers in different laboratories will increasingly pool their data.

The present paper has been written primarily for industrial infra-red spectroscopists. However, the results should be useful also to others. In particular, the theory presented should make it possible in some cases to derive, from the variation of the observed extinction with the experimental parameters, information about band structure which is not revealed directly by the spectrometer used.

We have limited ourselves to cases where collision damping is the chief cause of line-broadening. With strongly polar or reactive gases, much greater deviations from the simple absorption laws are to be expected and have in certain cases been observed. In such cases, the conditions for analysis of mixtures by infra-red absorption spectra are less favorable. On the other hand, the infra-red spectrum of such a mixture is a valuable source of information about intermolecular forces.

In conclusion, we wish to express our appreciation to Mr. L. H. Berryman for his help in preparing the figures. The senior author gratefully acknowledges a grant from the University of Oklahoma Faculty Research Fund.

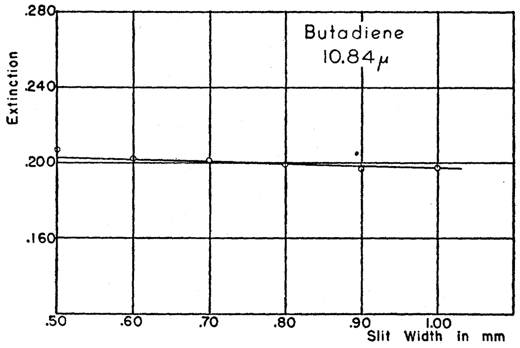

FIG. 21. Variation with slit width of the extinction of butadiene at 10.84μ ("*R*-branch").

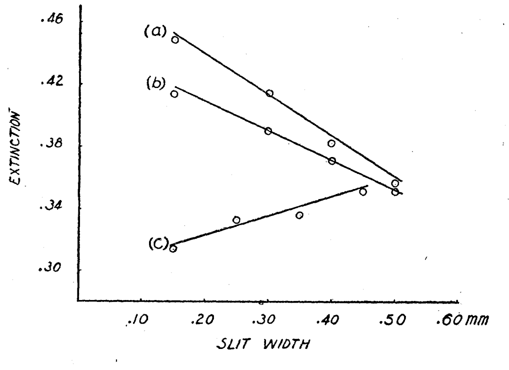

FIG. 22. Variation with slit width of the extinction of butadiene for three spectrometer settings in the 6.26μ double band. (a) 6.22μ pressure 157.0 mm, cell 2.00 cm; (b) 6.29μ pressure 160.7 mm, cell 2.00 cm; (c) 6.26μ pressure 170.7 mm, cell 2.00 cm.

BIBLIOGRAPHY

(1) Cf. P. Bouguer, *Traite d'Optique*, 1760.
(2) A. v. Beer, Pogg. Ann. **86**, 78 (1852).
(3) K. Angström, Öfversigt af K. Vetensk. Akad. Förh. **46**, 549 (1889).
(4) K. Angström, Öfversigt af K. Vetensk. Akad. Förh. **47**, 331 (1890).
(5) K. Angström, Phys. Rev. **1**, 597 (1892).
(6) K. Angström, Ann. d. Physik **6**, 163 (1901).
(7) K. Angström, Arkiv f. Matematik, Astronomi och Fysik **4**, No. 30 (1908).
(8) Cl. Schaefer, Ann. d. Physik **16**, 93 (1905).
(9) H. Rubens and E. Ladenburg, Verh. d. D. Phys. Ges. **7**, 170 (1905).
(10) J. Koch, Öfversigt af K. Vetensk. Akad. Förh. **58**, 331 (1901).
(11) Eva v. Bahr, Ann. d. Physik **29**, 780 (1909).
(12) Eva v. Bahr, Ann. d. Physik **33**, 585 (1910).
(13) Eva v. Bahr, Physik. Zeits. **12**, 1167 (1911).
(14) Eva v. Bahr, Verh. d. D. Phys. Ges. **15**, 673 (1913).
(15) Eva v. Bahr, Verh. d. D. Phys. Ges. **15**, 710 (1913).
(16) C. Füchtbauer, Physik. Zeits. **12**, 722 (1911).
(17) H. A. Lorentz, Proc. Amst. Acad. Soc. **8**, 591 (1906).
(18) G. Hertz, Verh. d. D. Phys. Ges. **13**, 617 (1911).
(19) M. Wimmer, Ann. d. Physik **81**, 1091 (1926).
(20) W. Lasareff, Zeits. f. Physik **64**, 598 (1930).
(21) W. Grasse, Zeits. f. Physik **89**, 261 (1934).
(22) P. C. Cross and Farrington Daniels, J. Chem. Phys. **2**, 6 (1934).
(23) G. Becker, Zeits. f. Physik **34**, 255 (1925).
(24) D. G. Bourgin, Phys. Rev. **29**, 794 (1927).
(25) H. Becker, Zeits. f. Physik **59**, 583 (1930).
(26) R. M. Badger and J. L. Binder, Phys. Rev. **37**, 800 (1931).
(27) G. Herzberg and J. W. T. Spinks, Proc. Roy. Soc. **A147**, 434 (1934).
(28) S. D. Cornell and W. W. Watson, Phys. Rev. **50**, 279 (1936).
(29) S. D. Cornell, Phys. Rev. **51**, 739 (1937).
(30) H. W. Kussmann, Zeits. f. Physik **48**, 831 (1928).
(31) J. Kühne, Zeits. f. Physik **84**, 722 (1933).
(32) R. R. Brattain, R. S. Rasmussen and A. M. Cravath, J. App. Phys. **14**, 418 (1943).

(33) R. B. Barnes, U. Liddel and V. Z. Williams, Ind. Eng. Chem. (Anal. Ed.) **15**, 659 (1943).
(34) R. B. Barnes, R. C. Gore, U. Liddel, and V. Z. Williams, *Infrared Spectroscopy* (Reinhold Publishing Corporation, New York, 1944).
(35) G. L. Gouy, Comptes rendus **88**, 418 (1879).
(36) Lord Rayleigh, Phil. Mag. **27**, 298 (1889).
(37) M. Planck, Sitz. d. K. Akad. D. Wiss. zu Berlin **1**, 370 (1903).
(38) M. Planck, Sitz.-Preuss. Akad. Wiss. **1**, 480 (1903).
(39) W. C. Mandersloot, Jahrb. d. Radioakt. **13**, 1 (1916).
(40) J. Holtsmark, Ann. d. Physik **58**, 577 (1919).
(41) J. Holtsmark, Zeits. f. Physik **34**, 722 (1925).
(42) L. Mensing, Diss. Hamburg (1925).
(43) V. Weisskopf and E. Wigner, Zeits. f. Physik **63**, 54 (1930).
(44) V. Weisskopf, Physik. Zeits. **34**, 1 (1933).
(45) H. Margenau and W. W. Watson, Rev. Mod. Phys. **8**, 22 (1936).
(46) G. Hettner, Physik. Zeits. **27**, 787 (1926).
(47) R. Ladenburg and F. Reiche, Ann. d. Physik **42**, 181 (1913).
(48) D. M. Dennison, Phys. Rev. **31**, 503 (1928).
(49) L. A. Matheson, Phys. Rev. **40**, 81 (1932).
(50) C. L. Pekeris, Astrophys. J. **79**, 441 (1934).
(51) W. M. Elsasser, Phys. Rev. **54**, 126 (1938).
(52) M. Summerfield and John Strong, Phys. Rev. **59**, 217 (1941).
(53) M. Summerfield and John Strong, Phys. Rev. **60**, 162 (1941).
(54) John Strong, J. Frank. Inst. **232**, 1 (1941).
(55) W. M. Elsasser, Phys. Rev. **53**, 768 (1938).
(56) F. Paschen, Ann. d. Physik **60**, 661 (1897).
(57) C. Eckart, Phys. Rev. **51**, 735 (1937).

Erratum: Sound Waves in Rooms

Philip M. Morse and Richard H. Bolt

[Rev. Mod. Phys. **16**, 69 (1944)]

ADD to the last paragraph of Section 20 the following sentences and equation:

For instance, for wave-lengths long compared to the thickness of material plus air backing, the wall impedance is approximately that of two equivalent circuit arms in parallel, the impedance of the two arms being

$$\left.\begin{array}{c} r_nL+(i\rho c^2/\omega PL) \text{ and } r_nL+(i\rho c^2/\omega L_aB_a) \\ \text{where } B_a \simeq \begin{cases} 1, & \text{Transverse waves suppressed} \\ \cos\varphi_1, & \text{Transverse waves allowed} \end{cases} \end{array}\right\}. \qquad 4.15$$

This corresponds approximately to the circuit in Fig. 8a. In the present instance it is somewhat more accurate to insert a resistance in both arms and to neglect the inductance. The third arm, corresponding to panel motion, will be discussed in the next section.

Erratum: Surface Roughness and Sliding Friction

J. J. Bikerman

[Rev. Mod. Phys. **16**, 53 (1944)]

ON page 63, in the second paragraph in the left-hand column, (Section II, 6) should be (Section II, 2, b3).